Long term properties of geoelectrical monitoring system installations in embankment dams in Sweden

T. Dahlin
Engineering Geology, Lund University, Lund, Sweden

P. Hedblom
Engineering Geology, Lund University, Lund, Sweden

P. Sjödahl
HydroResearch AB, Täby, Sweden

ABSTRACT: The demand for better methods for condition control and monitoring of embankment dams is increasing due to ageing and higher demands on availability. Electrical resistivity tomography (ERT) can be used to monitor the interior of the dam to detect flow-induced variation in the resistivity caused by temperature, dissolved solids and grain size changes. In Sweden electrodes for ERT were installed in embankment dams at 4 hydropower plants between 1999 and 2007, where 3 of them included electrodes intended for self-potential (SP) as well as ERT potential measurements. For two of the dams the electrode installations have been used for ERT monitoring continuously since the installation, whereas for the other two they were only used during a part of the period. An important question for the applicability of geoelectrical monitoring of dams is the long-term quality of the electrode installation, since long time series of data of comparable quality are essential for allowing to identify long term changes in the properties of the embankment dam. To assess the quality of the electrode installations measurement technical tests were carried out on the 4 dams during 2022. The tests were made with state-of-the-art instrumentation as well as a research prototype instrument, and include electrode contact resistances, full waveform data with high dynamic and temporal resolution, reciprocal data for observation error calculations and passive noise measurements. The results show that the stainless-steel electrodes for ERT retain good properties and result in good data quality, whereas the non-polarisable (Cu-$CuSO_4$) electrodes are problematic with very high contact resistances for many of them. Furthermore, the electrode cables are of inadequate quality for one of the dams, which lead to damage during the installation with loss of electrodes and eventually short-circuiting. For the other 3 dams the cables are apparently intact and continue to provide good quality data.

1 INTRODUCTION

1.1 *Background*

Electrical resistivity tomography (ERT) can provide spatial information in the interior of the dam core if the electrode spreads are installed adjacent to it. ERT has been tested as a monitoring method in a number of Swedish dams, with electrodes installed along the top of the core (e.g. Sjödahl et al. 2009; Sjödahl et al. 2008; Dahlin et al. 2001; Johansson & Dahlin 1996). It has the advantage of focusing the sensitivity of the measurements to the dam core and can thereby provide valuable information even if the resistivities and depths will be distorted by so called 3D effects if not handled in the inversion of the data (Sjödahl et al. 2006).

The measurements of direct current (DC) resistivity can be expanded to include time-domain induced polarisation (IP), which often is referred to as DCIP tomography (Binley & Slater 2020). The IP effect, often expressed as chargeability, is related to the pore structure of the material. The IP effect can provide additional information that may in some cases resolve ambiguities in the resistivity parameter, and under certain conditions provide information on the hydraulic conductivity (Maurya et al. 2018).

1.2 *Aim and purpose*

The aim of the study was to achieve knowledge about the long-term performance of electrode installations as part of a system for detecting internal defects and processes in embankment dams which can potentially threaten the stability of these. Furthermore, to learn about the characteristics of typical electrical noise signals that contaminate ERT / DCIP data acquired at such sites.

The purpose was to carry out test measurements on the electrode installations at the four embankment dams in a systematic way, and to analyse the resulting data in terms of data quality related parameters for resistivity and IP measurements, and to measure and analyse noise signals.

2 METHOD

2.1 *Active measurements*

Preparations for the test measurements were made by creating spread files that describe how the electrode layouts (spreads) are designed and wired to the instrument, and protocol files that define the measurement sequences to be used. The electrode arrays used vary between the embankment dams and spreads but multiple gradient array and a reciprocal version of it are included in all cases. For some of the electrode spreads extended gradient, dipole-dipole or pole-dipole array measurements were also done.

The end connectors of the existing electrode cables were connected to an ABEM Terrameter LS2 for each electrode spread. Electrode contact resistance was measured with the "focus-one" technique before the measurements started (Ingeman-Nielsen et al. 2016), using a small test current (1 mA) in consideration of the non-polarisable electrodes. The measurement tests were done with 100 % duty cycle IP mode (Olsson et al. 2015) using 2 s long pulses and 2 full measurement cycle stacks (+-+-). Maximum output voltage from the transmitter was limited to 400 V and the requested current was 200 mA, except for some repetition test rounds with reduced current.

The reciprocal data pairs were used to calculate observation errors on basis of the reciprocity theorem, which states that measurements made with transmitter and receiver positions reversed should give identical results unless there are measurement errors.

2.2 *Passive measurements*

Passive measurements were carried out when no active measurements were in progress to gain insight in the character of electrical noise at the sites.

A relay switch of type ABEM Electrode Selector ES10-64C was used to connect selected electrodes from one or two spreads to an 8-channel prototype DCIP receiver with 24 bit A/D converters developed by us. The receiver was set to record the voltage signals between the selected electrode pairs continuously for several hours, primarily outside office hours and overnight, with a sampling rate of 32 kHz.

Analyses of the spectral content of the signals were done in Matlab using Welch's power spectral density estimate (pwelch). Two time periods of 54 seconds each (~$1.7 \cdot 10^6$ samples) were selected from the several hours long continues recording. The window time and the nFFT were set to 2^{17} (131 072) with no overlap, resulting in 0.2 Hz wide FFT bins.

3 SITE DESCRIPTIONS

3.1 *Electrode installations*

Electrode spreads were installed in four Swedish embankment dams during the period 1999 to 2007, all being designed and built as zoned embankment dams, as summarised in Table 1. A combination of stainless-steel plates and non-polarisable electrodes were used, where the latter were intended for self-potential (SP) as well as ERT potential measurements, except for one of the dams where only steel plates were installed. The steel electrodes consist of 250 mm x 250 mm x 0.5-1.0 mm plates of acid grade stainless-steel, which are joined to a multi-stranded stainless steel wire with polyurethane (PUR) jacket by bending one corner of the plate over a stripped portion of the wire and fixing it with some hammer blows. The PUR covered wire was joined to pig-tail outlets on a multi-core cable with PUR jacket using a crimp cylinder, and the joint was insulated with heat-shrink using a generous amount of melt glue. This was complemented with self-vulcanising tape, to ascertain a waterproof connection to prevent corrosion caused by a combination of different metals being exposed to moisture. Farwest Corrosion Control SP-150 Cu-$CuSO_4$ non-polarisable reference electrodes were delivered pre-packaged in a bag with a bentonite mixture intended to ensure good electrode contact after soaking with water at the installation. The electrode cables were tailor made by manufacturers that supply the oil and gas industry with seismic survey cables. The cables have heavy duty PUR jacket suitable for permanent burial underground in water saturated conditions, except for one of the sites where the cables are less ruggedised.

Figure 1. Installation of a) stainless steel plate electrode, b) non-polarisable electrode (Cu-$CuSO_4$ pre-packaged in bentonite mixture).

Automatic long-term ERT monitoring has been carried out for various durations on the installed electrodes, with resulting data that varied in quality between the sites.

Table 1. Summary of dam installations (SS = stainless steel plate and NP = non-polarisable).

Installation characteristics	Dam 1	Dam 2	Dam 3	Dam 4
Dam length [m]	210+410	120+200	140	150
Maximum dam height [m]	32	30	25	9
Electrode placement	Top of core	Top of core, u/s slope & d/s toe	Top of core & d/s slope	Top of core, u/s & d/s filter
Year of installation	1999	(1996) 2005	2006	2007
Monitoring period	2001-2009	1996-2005 and 2006-ongoing	2007-ongoing	2019-2022
Type of electrodes	SS and NP	SS and NP	SS	SS and NP
Electrode spacing [m]	3-6	3.5-7	2	2.5
Installed spreads / lines	2	5	2	3
No of electrodes	58+64	32+54+24+17+19	41+64	60+34+34
Type of measurements	ERT, IP & SP	ERT, IP & SP	ERT & IP	ERT, IP & SP
Existing / New dam	Existing	Existing	Existing	New

3.2 *Dam 1*

The embankment dam consists of a 210 m main dam with a maximum height of 32 m, and a 410 m long lower side dam. Electrode layouts were installed in the upper part of the dam core in connection with the raising of it during the summer of 1999. Stainless steel electrodes were placed with a mutual distance of 6 meters along the crest of the main dam and the side dam, and in addition non-polarisable electrodes were installed along the dam crest with the same mutual distance but with an offset of 3 meters relative to the steel electrodes. A sensor for water resistivity and temperature sensors was installed in the reservoir and connected to the ERT instrument. Monitoring with automated ERT was carried out during 8 years starting in May 2001.

3.3 *Dam 2*

The embankment dam is divided into a left and a right part with a centrally placed power plant and spillway structure. Electrode layouts were installed in the upper part of the dam core in connection with the raising of it during the summer of 2005, replacing older electrode installations from 1996 that were removed. Electrodes in the form of stainless steel plates were placed with a mutual distance of 7 m along the left and right dam crests, and in addition non-polarisable electrodes were installed there with the same mutual distance but with an offset of 3.5 m relative to the steel electrodes. There are in total 32 electrodes on the left and 54 on the right crest. Furthermore, an underwater electrode cable with 24 built-in stainless steel cylinder electrodes was deployed along the upstream side of the left dam. On the right dam electrode cables originally installed along the downstream toe and in the reservoir on the upstream side in 1996 were removed before the construction works started and re-installed afterwards. There are 19 electrodes on the right downstream side and 17 on the upstream side, in both cases with a separation of 7 m. A probe for water resistivity and temperature was placed hanging in the intake for connection to the ERT instrument.

Monitoring with automated daily measurements on the original electrode installation took place between autumn 1996 and spring 2005. Monitoring with the present electrode spreads started in March 2006 and is still in progress, including resistivity and IP.

3.4 *Dam 3*

The dam is 140 m long with a maximum height around 25 m. Electrode layouts were installed along the dam crest in connection with raising the dam core during the summer 2006. Another line of electrodes was installed in the support fill along the downstream slope. The crest layout consists of 41 and the downstream layout of 64 electrodes, all with 2 m spacing and in the form of stainless steel plates throughout.

Monitoring with automated daily measurements is in progress since December 2007 and includes resistivity and IP.

3.5 *Dam 4*

A new 9 m high and 150 m long embankment dam was built in 2007. Along the top of the dam core 60 electrodes were installed. Another two lines of 34 electrodes each were installed in the upstream and downstream filter just above the foundation level. Hence 128 electrodes in total with a spacing of 2.5 m throughout, where every second electrode is a stainless steel plate and every second is non-polarisable.

Notable is that the installation depth is much larger for the electrodes installed in the filters compared to the other installations. Moreover, the electrode cables used at Dam 4 have much thinner jacket than at the other test sites, probably due to glitches in the communication with the cable manufacturer during the purchase process.

Continuous monitoring was done 2019-2022.

4 RESULTS AND DISCUSSION

4.1 *Electrode contact resistance*

The electrode contact resistance gave stable and repeatable results despite the small test current (1 mA). The stainless steel electrodes have low to medium contact resistances (a few hundred to some thousand **Ω**) throughout (Table 2). Notice that Dam 2 left upstream side exhibit the highest resistances among the steel electrodes despite that they lie submerged in the reservoir. This can be explained by the high resistivity (low conductivity) of the reservoir water and a relatively small surface area of the electrodes. The electrodes on Dam 2 right upstream side have a different design with larger surface area, which results in lower contact resistances. The steel electrodes generally appear to be in good condition with all being functional for Dam 2 and Dam 3, one only with damaged connection for Dam 1 but with 7 damaged for Dam 4.

The non-polarisable electrodes exhibit higher contact resistances for all layouts, which for the Dam 2 and Dam 1 crests are around an order of magnitude higher. It is not known if the high contact resistances are caused by drying out of the $CuSO_4$ in the electrodes, or if the wetting of the bentonite mix they were installed in was insufficient for those. Similar electrodes should be soaked with at least around 20 litres of water each according to the instructions, and it may be questioned if so much water was used throughout. The instruments used at the time of the installations did not offer a possibility to measure the electrode contact resistances in a way that is comparable with the modern instrument, hence no such data exists from the time of installations, although thorough measurement tests and analyses were made (Johansson et al. 2005). According to the manufacturer the design life of the electrode was 10 years, which means that these electrodes have passed their design life with margin for all the dams. It is furthermore complicating for the data quality assessment that the non-polarisable electrodes are not to be used for current transmission, thus preventing reciprocal error evaluation that is the most reliable method for quality assessment of the electrode function.

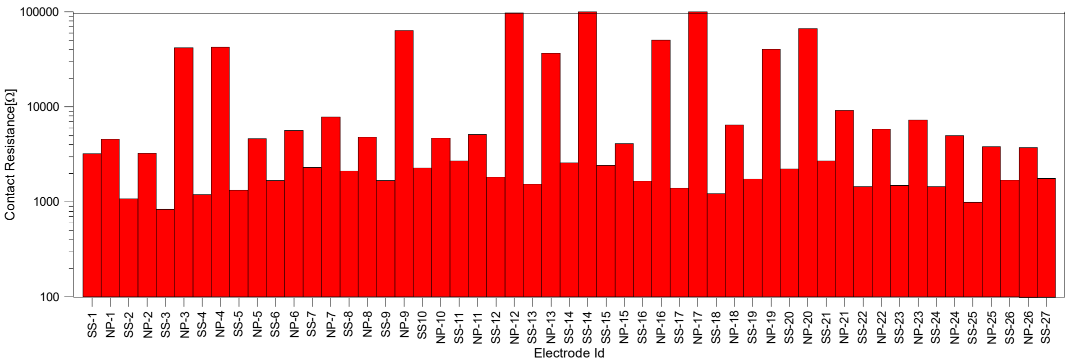

Figure 2. Example of electrode contact resistance test result, where NP labels are used for non-polarisable electrodes and SS for stainless steel electrodes.

At Dam 4 five of the non-polarisable electrodes have damaged connection. Furthermore, 18 of the upstream side bottom electrodes at Dam 4 have suspiciously low contact resistance (around 100 Ω). This together with an observation of measured potentials being in the same range as the output voltage from the transmitter suggests short-circuit in the electrode cable.

Results from Dam 2 right side crest is shown as example in Figure 2, notice the higher resistances for the non-polarisable (NP) compared to the stainless steel (SS) electrodes.

Table 2. Summary of electrode contact resistance test results.

Site and spread	No of electrodes	Contact resistance[Ω]			Comment
		Mean	Median	Std Dev	
Dam 1 main dam (SS)	28(29)	371	374	84	Stainless steel (1 broken)
Dam 1 main dam (NP)	29	41 158	11 508	60 407	Non-polarisable
Dam 1 side dam	64	349	344	49	Stainless steel
Dam 2 left crest (SS)	16	2 040	2 163	1 014	Stainless steel
Dam 2 left crest (NP)	16	86 890	70 408	92 990	Non-polarisable
Dam 2 right crest (SS)	27	1 799	1 680	589	Stainless steel
Dam 2 right crest (NP)	26	29 322	6 871	36 446	Non-polarisable
Dam 2 left upstream	24	5 198	5 129	254	Stainless steel
Dam 2 right upstream	17	2 020	2 004	179	Stainless steel
Dam 2 right downstream	19	4 485	4 482	1 829	Stainless steel
Dam 3 crest	41	605	576	243	Stainless steel
Dam 3 downstream	64	997	796	432	Stainless steel
Dam 4 crest (SS)	29(30)	798	791	118	Stainless steel (1 broken)
Dam 4 crest (NP)	29(30)	1 609	1 022	2 810	Non-polarisable (1 broken)
Dam 4 bottom (SS)	27(34)	472	444	358	Stainless steel (7 broken)
Dam 4 bottom (NP)	30(34)	1 179	1 145	1 317	Non-polarisable (4 broken)

There was no sign of the water resistivity and temperature probes at dam 1 and Dam 2.

4.2 *Reciprocal error analysis*

The measurement errors were quantified from reciprocal data pairs using multiple gradient array, a so called nested array where all potential electrode pairs are in between the current electrodes. In some cases the measurement sequence was extended with measurements outside the current electrodes as well.

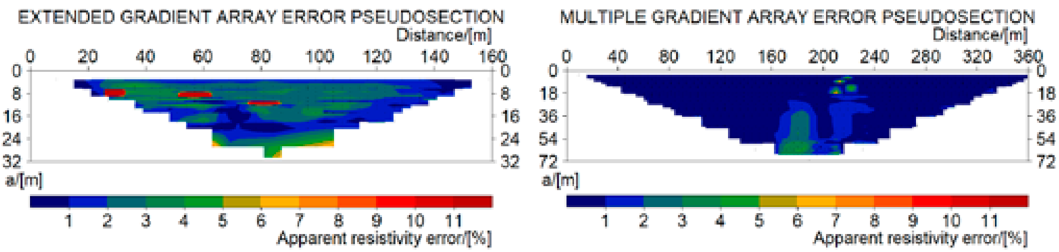

Figure 3. Examples of reciprocal error pseudosections for measured apparent resistivity from Dam 1.

Error pseudosections for resistivity from Dam 1 crest and side dam are shown as examples in Figure 3, based on reciprocal data pairs from extended gradient array and multiple gradient array respectively. The 3 outliers for the crest are caused by the reciprocal non-nested arrays which are more susceptible to noise due to the lower signal levels and large separation between the potential electrodes, and they are not present for the nested array data (see Table 3). Apart from these the errors lie within few percent for the apparent resistivity (Figure 3).

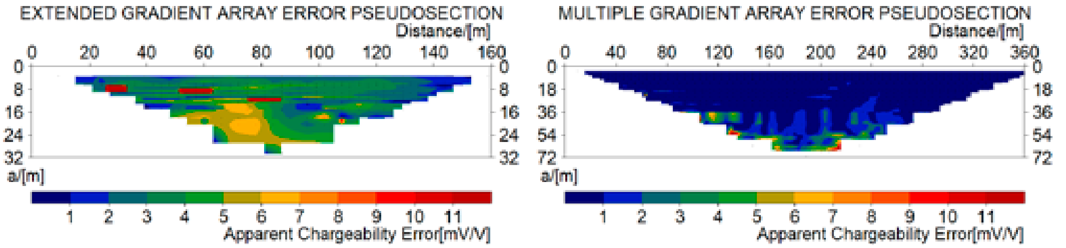

Figure 4. Examples of reciprocal error pseudosections for IP effect expressed as integral apparent chargeability (10 -1990 ms) from Dam 1.

The corresponding error for the IP effect, based on integral chargeability, are well under 10 mV/V with a few exceptions, as shown in the pseudosections in Figure 4.

Table 3. Summary of reciprocal error test results, where the apparent chargeability values are based on integral chargeability (10 -1990 ms). All measurements were done on the stainless steel electrodes only.

Site and spread	No of data	Resistivity errors[%]			Chargeability errors[mV/V]		
		Mean	Median	StdDev	Mean	Median	StdDev
Dam 1 main dam (nested)	198	2.08	2.07	1.19	3.2	3.15	1.46
Dam 1 main dam (all)	409	3.62	2.16	16.91	$2.3 \cdot 10^3$	3.09	$4.5 \cdot 10^4$
Dam 1 side dam	1373	0.44	0.18	0.99	0.69	0.18	1.89
Dam 2 right crest (nested)	189	13.57	3.58	26.17	46.49	1.27	486.91
Dam 2 right crest (all)	389	11.88	4.32	24.56	26.04	1.33	340.23
Dam 2 left crest	48	11.38	3.69	17.61	5.58	2.18	11.26
Dam 2 left upstream	147	0.28	0.19	0.37	1.28	0.63	2.12
Dam 2 right upstream	56	0.09	0.06	0.08	0.22	0.18	0.18
Dam 2 right downstream	76	5.54	0.26	30.59	7.7	0.31	47.88
Dam 3 crest	518	1.91	1.14	2.19	1.2	0.82	1.22
Dam 3 downstream	1372	3.36	1.24	7.84	22.04	0.87	768.04
Dam 4 crest	216	163.91	75.25	293.34	146.96	55.51	257.64
Dam 4 bottom	26	83.25	11.91	282.18	15.29	5.64	19.33

4.3 *Inverse numerical modelling*

Inverted models based on the normal datasets behind the error sections displayed in Figure 3 and Figure 4 are shown in Figure 5 and Figure 6 respectively. Both the resistivity and chargeability (IP effects) yield inverted models with small residuals, which is a manifestation of good data quality.

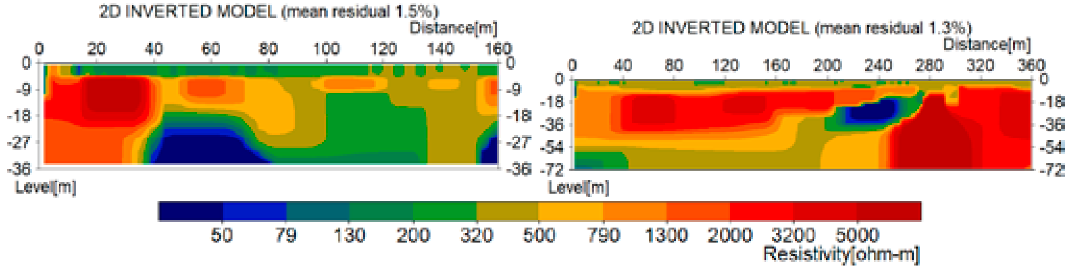

Figure 5. Examples of inverted resistivity sections from Dam 1.

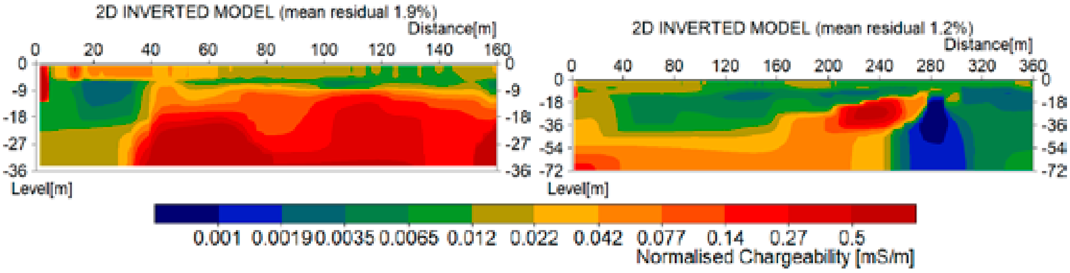

Figure 6. Examples of inverted normalised chargeability sections from Dam 1.

4.4 *Background signal noise characteristics*

The background noise was measured in 8 simultaneous channels between a number of selected electrodes distributed along the spreads, at varying separations in the range 14-98 m. The signal varies in time and along the electrode layouts and reach to above 2.5 V peak amplitude for some channels (Figure 7). In some cases there is a clear correlation between the noise level and the production, as in the example in Figure 7 where the production was stopped at 22:30 and re-started at 04:00. There is however also noise that does not seem to be coupled with the production at the plant but possibly comes from the power grid, like between 01:00 and 04:00. The increase in noise level at 07:30 coincides with the start of ERT measurements.

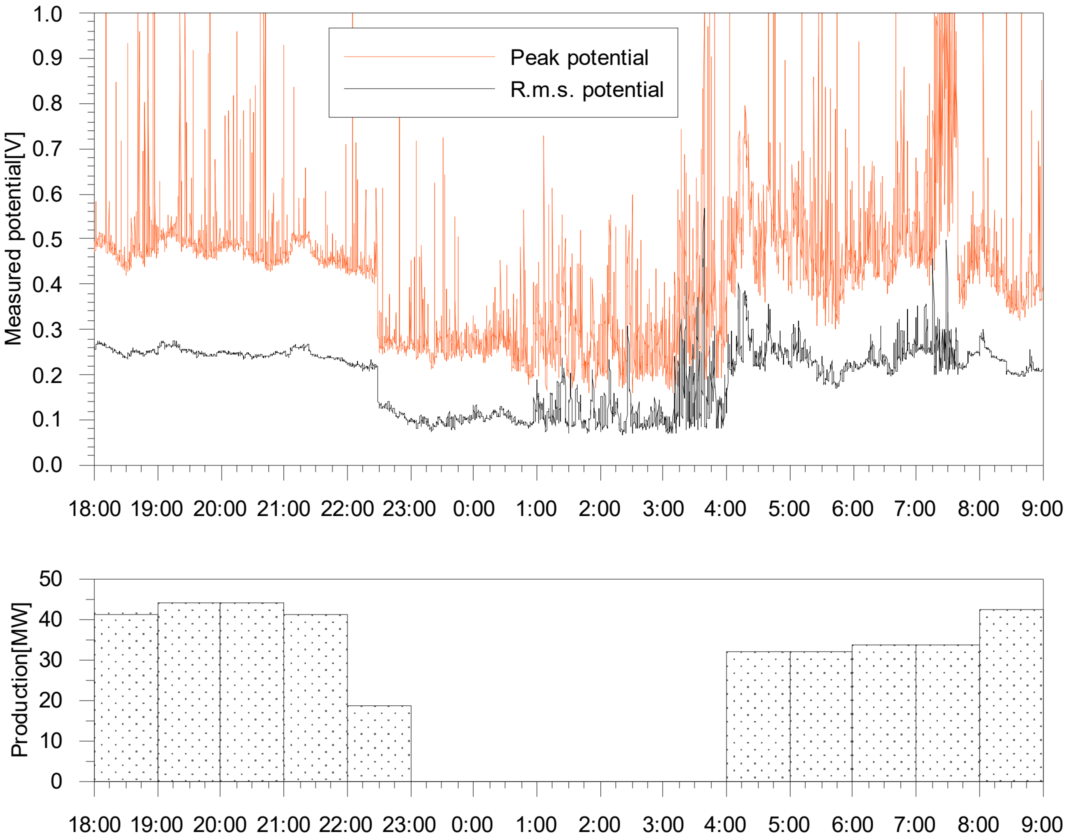

Figure 7. Example of overnight noise recording between two installed electrodes inside the crest of Dam 2 (upper) and the corresponding power production at the plant (lower).

The noise is dominated by 50.0 Hz and harmonics (Figure 8), plus a smaller peak for 16.6 Hz during production which suggests that the railway power supply system affects the noise spectrum. The noise contains frequencies over several kHz at significant levels, which has implications for the design of the input section of instruments to be used for ERT/DCIP on such sites.

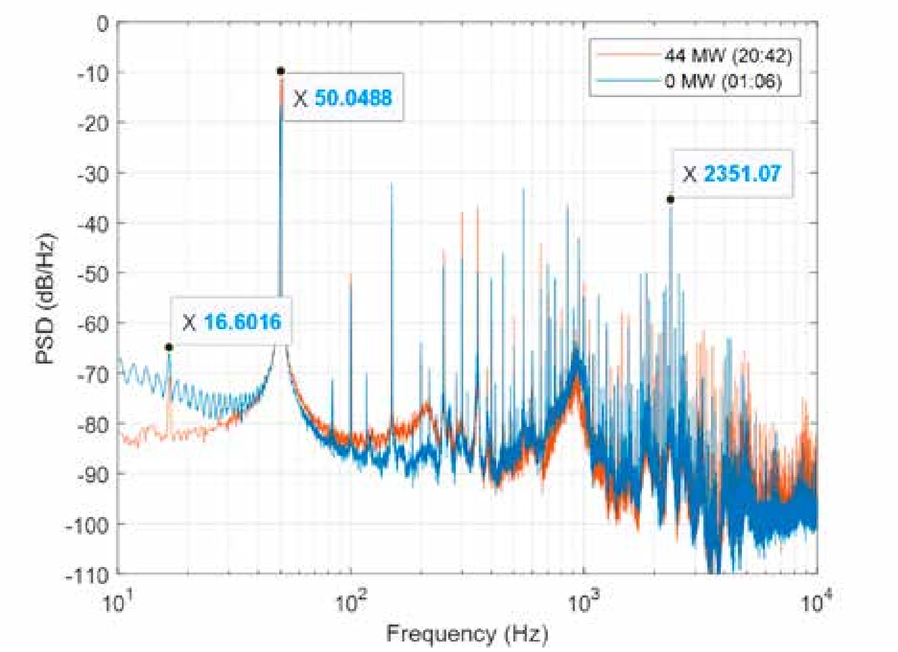

Figure 8. Example of frequency content in signals recorded in Dam 2 in data extracted from the time series displayed in Figure 7.

5 CONCLUSIONS

The results show that the majority of the stainless steel electrodes retain good properties with low to moderate contact resistance, and result in good data quality 15-23 years after the installation. Apart from at Dam 4, where problems were evident in connection with the installations, only one electrode has become useless due to some unknown type of damage. The non-polarisable (Cu-$CuSO_4$) electrodes are, however, problematic with very high contact resistances for many of them. It is not known if the high contact resistances are caused by drying out of the $CuSO_4$ in the electrodes, or if the wetting of the bentonite mix during the installation was insufficient, but the expected design life for them has passed. Furthermore, it is complicating for the data quality assessment that the non-polarisable electrodes are not designed for current transmission, thus preventing reciprocal error evaluation. Hence only stainless steel electrodes are recommended for long-term monitoring installations of ERT or DCIP.

The results highlight that the quality of the electrode cables and care with details in the installation process are essential. The cables are of inadequate quality at Dam 4, which lead to damage during the installation with loss of electrodes and as it appears continued degradation eventual short-circuiting. For the other 3 dams the cable installations are apparently intact and continue to provide good quality data.

For future installations for monitoring with ERT or DCIP it is recommended to follow the same type of installation procedure as was done for the surveyed dams but make certain to purchase cables that are designed for permanent burial under partially or fully water saturated condition. Non-polarisable electrodes similar to the type used here should be avoided, unless proven functional by long term testing. The mechanical strength of the cable and the connections must withstand the handling when burying them in the embankment dam, and the connection points between different metals must be securely sealed against water ingress to avoid corrosion.

The probes for measuring water resistivity and temperature in the reservoir need to be robust and easy to install for deployment and survival in typical embankment dam environments, and they need to be designed for the very low conductivities (high resistivities) that are typical for Swedish conditions. This may be challenging to find on the market.

The noise recordings show that there are noise components between 16.6 Hz and several kHz that need to be considered for DCIP instrument design and signal processing.

6 ACKNOWLEDGEMENTS

The study was carried out within the framework of Swedish Centre for Sustainable Hydropower - SVC (project VKU32020). SVC has been established by the Swedish Energy Agency, Energiforsk and Svenska Kraftnät together with Luleå University of Technology, KTH Royal Institute of Technology, Chalmers University of Technology, Uppsala University and Lund University (http://www.svc.nu). We wish to thank the embankment dam owners and their staff for access to the sites and support in connection with the test measurements.

7 REFERENCES

Binley A., & Slater L. (2020) *Resistivity and Induced Polarization: Theory and Applications to the Near-Surface Earth*. Cambridge: Cambridge University Press, ISBN 978-1-108-49274-4.

Dahlin, T., Sjödahl, P., Friborg, J. & Johansson, S. (2001) Resistivity and SP Surveying and Monitoring at the Sädva Embankment Dam, Sweden, in *Dams in a European Context, ed. G.H. Mistømme, B. Honningsvåg, K. Repp, K.A. Vaskinn & T. Westeren,* ISBN 90 5809 196 1, Balkema, Lisse, p.107-113.

Ingeman-Nielsen T., Tomaškovičová S. & Dahlin T. (2016) Effect of electrode shape on grounding resistances - Part 1: The focus-one protocol, *Geophysics*, 81(1), WA159-WA167.

Johansson, S., Friborg, J., Dahlin, T. & Sjödahl, P. (2005) *Long Term Resistivity and Self Potential Monitoring of Embankment Dams – Experiences from Dam 2 and Sädva Dams, Sweden*, Report 05:15, Elforsk, Stockholm, 123p.

Johansson, S. & Dahlin, T. (1996) Seepage monitoring in an earth embankment dam by repeated resistivity measurements, *European Journal of Engineering and Environmental Geophysics*, 1(3), 229-247.

Maurya P.K., Balbarini N., Møller I., Rønde V., Christiansen A.V., Bjerg P.L., Auken E. & Fiandaca G. (2018) Subsurface imaging of water electrical conductivity, hydraulic permeability and lithology at contaminated sites by induced polarization. *Geophysical Journal International*, 213(2), 770–785.

Olsson P.-I., Dahlin T., Fiandaca G. & Auken E. (2015) Measuring time domain spectral induced polarization in the on-time – decreasing the acquisition time and increasing the signal levels, *Journal of Applied Geophysics*, 123, 316-321.

Sjödahl P., Dahlin T. & Johansson S. (2009) Estimating seepage flow from resistivity monitoring data at the Sädva embankment dam, *Near Surface Geophysics*, 7, 463-474.

Sjödahl, P., Dahlin, T., Johansson, S. & Loke, M.H. (2008) Resistivity monitoring for leakage and internal erosion detection at Dam 2 embankment dam, *Journal of Applied Geophysics*, 65: 155–164.

Sjödahl, P., Dahlin, T. & Zhou, B. (2006) 2.5D Modelling to Assess 3D Effects in Resistivity Imaging on Embankment Dams, *Geophysics*, 71(5), G107-G114.